APL Materials

Electric field effects in graphene/$LaAlO_3$/$SrTiO_3$ heterostructures and nanostructures

Cite as: APL Mater. **3**, 062502 (2015); https://doi.org/10.1063/1.4916098
Submitted: 02 February 2015 • Accepted: 12 March 2015 • Published Online: 20 March 2015

Mengchen Huang, Giriraj Jnawali, Jen-Feng Hsu, et al.

Electric field effects in graphene/$LaAlO_3$/$SrTiO_3$ heterostructures and nanostructures

Mengchen Huang,[1] Giriraj Jnawali,[1] Jen-Feng Hsu,[1] Shonali Dhingra,[1] Hyungwoo Lee,[2] Sangwoo Ryu,[2] Feng Bi,[1] Fereshte Ghahari,[3] Jayakanth Ravichandran,[3] Lu Chen,[1] Philip Kim,[3] Chang-Beom Eom,[2] Brian D'Urso,[1] Patrick Irvin,[1] and Jeremy Levy[1,a]

[1]*Department of Physics and Astronomy, University of Pittsburgh, Pittsburgh, Pennsylvania 15260, USA*

[2]*Department of Materials Science and Engineering, University of Wisconsin-Madison, Madison, Wisconsin 53706, USA*

[3]*Department of Physics, Harvard University, Cambridge, Massachusetts 02138, USA*

(Received 2 February 2015; accepted 12 March 2015; published online 20 March 2015)

We report the development and characterization of graphene/$LaAlO_3$/$SrTiO_3$ heterostructures. Complex-oxide heterostructures are created by pulsed laser deposition and are integrated with graphene using both mechanical exfoliation and transfer from chemical-vapor deposition on ultraflat copper substrates. Nanoscale control of the metal-insulator transition at the $LaAlO_3$/$SrTiO_3$ interface, achieved using conductive atomic force microscope lithography, is demonstrated to be possible through the graphene layer. $LaAlO_3$/$SrTiO_3$-based electric field effects using a graphene top gate are also demonstrated. The ability to create functional field-effect devices provides the potential of graphene-complex-oxide heterostructures for scientific and technological advancement. [http://dx.doi.org/10.1063/1.4916098]

Two-dimensional graphene and complex-oxide interfaces possess properties that are of tremendous interest for fundamental science and future applications. Single-layer graphene (SLG) is a two-dimensional (2D) material with celebrated properties.[1–5] The quasi-two-dimensional interface between two insulating perovskite oxide semiconductors, $LaAlO_3$ (LAO) and TiO_2-terminated $SrTiO_3$ (STO), has also attracted intense interest in recent years[6] due to its unique electric-field-tunable properties, including conductivity,[7,8] superconductivity,[9,10] magnetism,[11–15] and spin-orbit coupling.[16,17] Recent reports have demonstrated that a variety of surface perturbations on $LaAlO_3$/$SrTiO_3$ (LAO/STO), including polar adsorbates,[18] metal layers,[19] metallic nanoparticles,[20] and other oxide layers,[21,22] can modulate the conductance at the interfacial two-dimensional electron gas (2DEG) between LAO/STO, indicating strong sensitivity of the conducting interface to the surface environment.

One unique property of LAO/STO heterostructures is the existence of a sharp metal-insulator transition (MIT) at a critical thickness[8] of approximately four unit cells of LAO. If the LAO layer is maintained to be slightly less than this critical thickness (~3 unit cells), the interface can be locally and reversibly switched between the conductive and insulating states using a conductive atomic force microscope (c-AFM) lithography technique.[23,24] Details of this procedure are described elsewhere.[25] This c-AFM lithography approach produces a wide range of nanodevices including field-effect transistors,[24,26] photodetectors,[27] terahertz emitters and detectors,[28] nanoscale rectifying junctions,[29] and single-electron transistors.[30]

The rich properties of both SLG and LAO/STO motivate efforts to create functional hybrid materials that combine the properties of both systems. Graphene has already been integrated with complex oxides[31] to create, for example, graphene/ferroelectric field effect transistors[32] and terahertz

[a]Author to whom correspondence should be addressed. Electronic mail: jlevy@pitt.edu

plasmonic devices.[33] Proximal coupling of graphene with LAO/STO heterostructures has the potential to create new functionality in each layer due to the small separation between the two layers (less than 2 nm for 3 unit cell LAO). Novel correlations are expected to develop between the coupled layers, possibly observable through transport. In addition, the unusual magnetic and superconducting properties of LAO/STO may interact in new and unexpected ways with the nearby graphene layer. Many practical devices may also be enabled by functional integration of these two materials. For example, LAO/STO interface can potentially serve as an ac ground plane capable of tuning the electrical properties of graphene and potentially reach a quantum-pressure driven regime of 2D plasmonic circuits[34] with potential applications in biosensing, large-molecule spectroscopy, and precision modulation.

LAO/STO heterostructures are fabricated by pulsed laser deposition. Approximately, 3 unit cells of LAO are grown on TiO_2-terminated STO (100) substrates, and *in situ* high pressure reflection high energy electron diffraction (RHEED) is used to control the LAO thickness. Details of the growth conditions and electrical contacting to the LAO/STO interface are described elsewhere.[35,36] SLG layers are deposited by mechanical exfoliation. After exfoliation, multi-layer and single layer graphenes are distributed on the 5 mm × 5 mm LAO surface. Figure 1(a) shows an optical micrograph of an area containing SLG. The four corners of the image are electrical contacts to the LAO/STO interface. Unlike graphene on SiO_2, graphene exfoliated on LAO/STO is barely visible under an optical microscope, and it is not possible to distinguish single-layer graphene from multi-layer graphene. Raman microscopy is used to identify SLG candidates by recording the characteristic G and 2D peaks (Fig. 1(b)). Once an area containing SLG is identified, the region is subsequently imaged using non-contact mode AFM (Fig. 1(c)) prior to c-AFM lithography. The height of SLG on LAO/STO is measured to be 0.6 nm from the AFM images, which is generally consistent with AFM results reported by other groups.[1,37]

C-AFM lithography is performed on the SLG/LAO/STO structures. "Virtual electrodes"[23] are created using a tip voltage V_{tip} = 15 V to form robust electrical contact to the oxide interface, followed by a straight line from one electrode to another (V_{tip} = 15 V, tip speed v_{tip} = 1000 nm/s) and intersecting the electrically isolated SLG region (Fig. 2(a)). All of the lithography procedures described in this paper are performed under ambient environmental conditions with a highly doped Si tip (spring constant k = 3 N/m). When the positively biased tip reaches the second electrode, the conductance abruptly increases (Fig. 2(b)), indicating that the c-AFM written area that overlaps the SLG is conductive. After writing, the nanowire is "cut" over the SLG region by applying a negative voltage to the tip (V_{tip} = −15 V) and slowly traversing the nanowire (v_{tip} = 10 nm/s) (Fig. 2(c)). As the tip passes over the nanowire, the conductance drops sharply to zero (Fig. 2(d)). By fitting the conductance profile,[23] an estimate for the nanowire width w = 18 nm is obtained. The conductance increase (~75 nS), non-exponential decay after writing, and estimated wire width are comparable to the results of c-AFM lithography on regular LAO/STO that does not contain graphene.[24,38] C-AFM

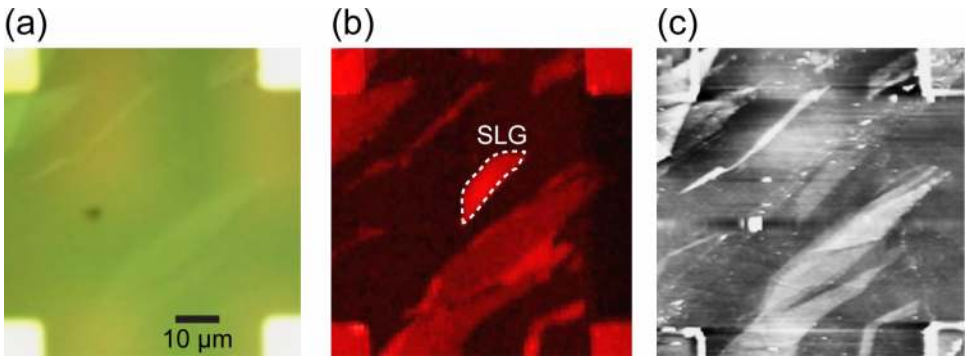

FIG. 1. Mechanical exfoliation of SLG on $LaAlO_3/SrTiO_3$ (SLG/LAO/STO). (a) Optical image of SLG/LAO/STO candidate. The four bright corners are Ti/Au electrodes contacting the LAO/STO interface. Multilayer graphene flakes can been seen but barely single layer. (b) Raman image at G-peak wave length, showing several SLG regions, one of which is identified by a white dashed boundary. (c) Non-contact AFM topography image of the same area.

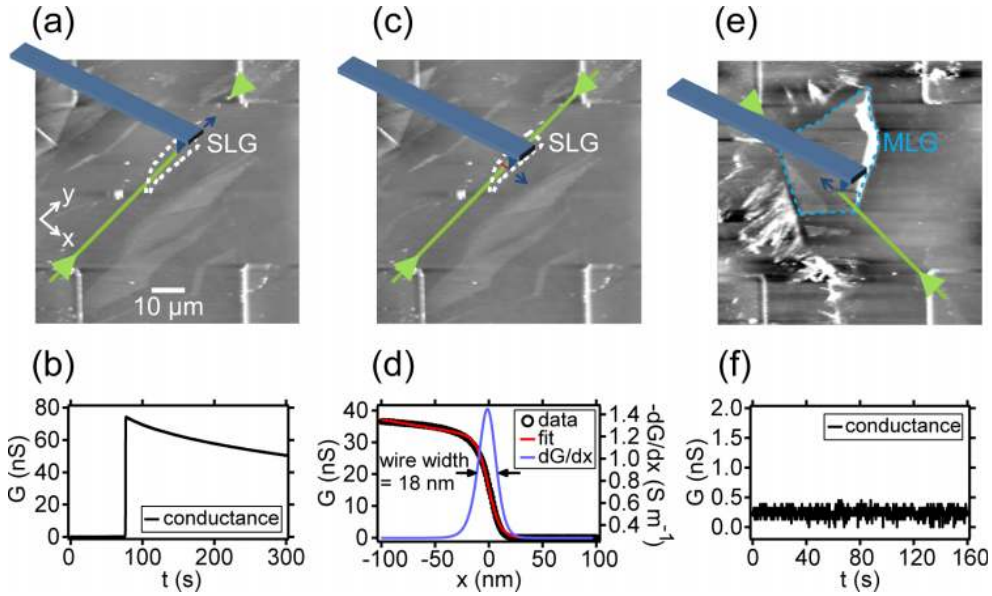

FIG. 2. C-AFM lithography on mechanically exfoliated SLG/LAO/STO. (a) A wire is written across the SLG region with $V_{tip} = 15$ V and $v_{tip} = 1000$ nm/s. (b) Conductance versus time between the two Ti/Au electrodes during the writing. The conductance abruptly increases when the positively biased tip reaches the second Au electrode. After writing, the conductance decays non-exponentially. (c) The existing wire is "cut" through the SLG region with $V_{tip} = -15$ V and $v_{tip} = 10$ nm/s. (d) Conductance versus position during the cut. The conductance drops to zero when the negatively biased tip moves across the wire. The conductance profile is fit using $G(x) = G_0 - G_1 \tanh(x/h)$. The deconvolved differential conductance dG/dx shows a full-width at half-maximum (FWHM) of 18 nm, which is used to quantify the width of the written wire. (e) Attempt to write through multilayer graphene (MLG) with $V_{tip} = 15$ V and $v_{tip} = 1000$ nm/s, along with (f) conductance profile during writing. No conductance increase is observed.

lithography with V_{tip} = 15 V is also performed on multilayer graphene (~4 nm thickness) covered area (Fig. 2(e)); however, no conductance jump (Fig. 2(f)) is observed.

One potential concern is that the c-AFM lithography may damage or chemically modify the graphene layer. To address this question, Raman spectroscopy is performed over regions that have been exposed to c-AFM lithography and compared with unexposed regions. The excitation laser (wavelength λ = 633 nm) is focused using a lens with numerical aperture NA = 1.4 to a spot size of $d \approx 550$ nm. The focused laser spot is scanned across the graphene region (Figure 3(a)). The step size between adjacent scans is 200 nm. Graphene and STO share spectral features in the range of 1200-1800 cm^{-1},[39] so subtraction from a region not containing graphene is required (Fig. 3(b)). A Lorentzian fit is performed to retrieve the peak position. A clear G peak at 1580 cm^{-1} and 2D peak with much stronger intensity at 2630 cm^{-1} is observed with no discernable D peak, supporting the claim that the SLG on LAO/STO is not measurably damaged by c-AFM lithography. Fig. 2(c) shows a sequence of Raman spectra taken over the path illustrated in Fig. 3(a). The G and 2D peak intensities decrease and eventually become zero as the laser spot moves out of the graphene layer. The spectra taken over the c-AFM exposed and unexposed areas are indistinguishable, and neither shows a measurable D peak, which is a sensitive measure for alteration of sp2 carbon bonding.

Although mechanical exfoliation is a simple way to transfer high-mobility SLG onto LAO/STO, there are many limitations to this approach. SLG on LAO/STO lacks optical contrast, forcing the use of time-consuming Raman mapping to identify suitable regions. To overcome these limitations, mm-scale SLG is grown by chemical vapor deposition (CVD) on ultraflat Cu substrates[40,41] and subsequently, transferred onto pre-patterned LAO/STO "canvases." Photolithography and oxygen plasma cleaning are used to selectively remove unwanted graphene; the remaining graphene is aligned with LAO/STO canvases with gold electrodes that independently contact the graphene on the surface and the LAO/STO interface.

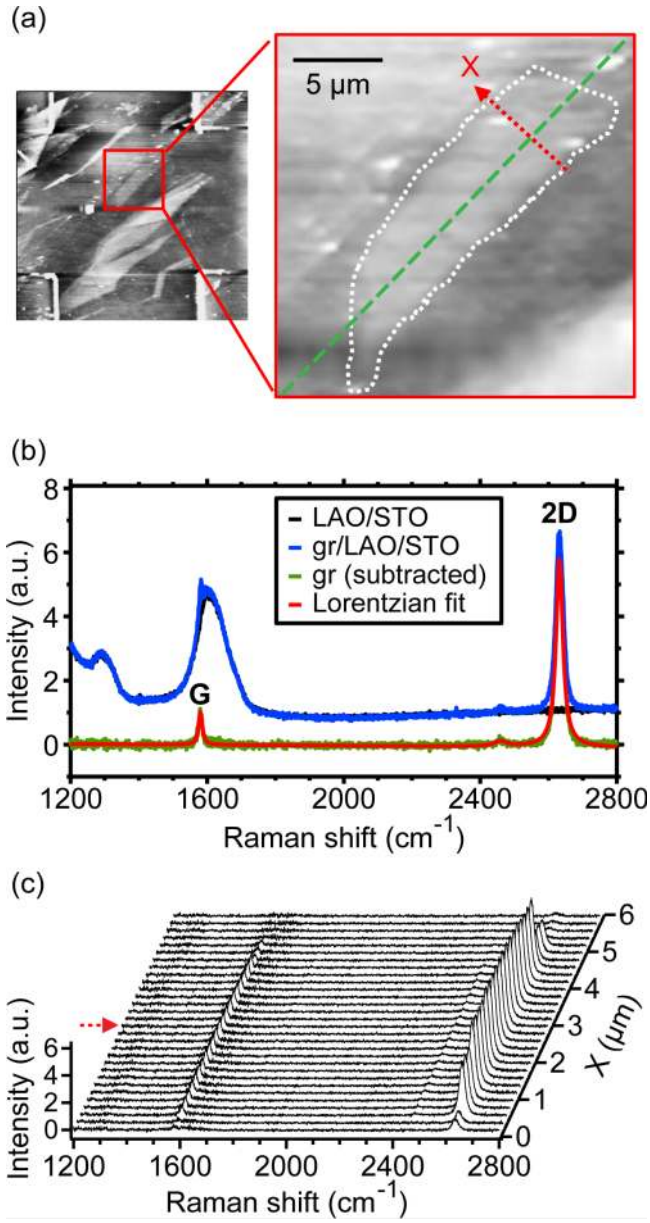

FIG. 3. Raman spectroscopy of exfoliated SLG/LAO/STO after c-AFM lithography. (a) Schematic showing the written wire (green dashed line) and the path (red dashed line with arrow) of the scanned Raman laser spot. (b) Representative Raman spectra data when the laser spot overlaps the wire previously created by c-AFM lithography (c) Raman spectra at different positions along the path "X" (indicated in Fig. 3(a)). The red arrow points out the representative data shown in Fig. 3(b).

C-AFM lithography performed on CVD SLG/LAO/STO shows that nanoscale control of the MIT through the SLG region can be performed in a manner similar to mechanically exfoliated SLG. Fig. 4(a) shows a region of a LAO/STO canvas that contains CVD-grown SLG. Unlike the experiments performed on exfoliated graphene, here, the graphene is electrically connected to an Au electrode. The two-terminal conductance, tip voltage, and graphene gate voltage are recorded as a function of time during the entire lithography procedure (Figure 4(b)). While writing the wire, the c-AFM tip is positively biased (V_{tip} = 20 V) and the graphene is grounded (V_g = 0 V). A conductance jump is observed when the wire path is finished. After writing, the graphene is kept grounded (V_g = 0 V) and the tip is held at V_{tip} = −15 V to cut the wire on graphene ("cut 1"). The

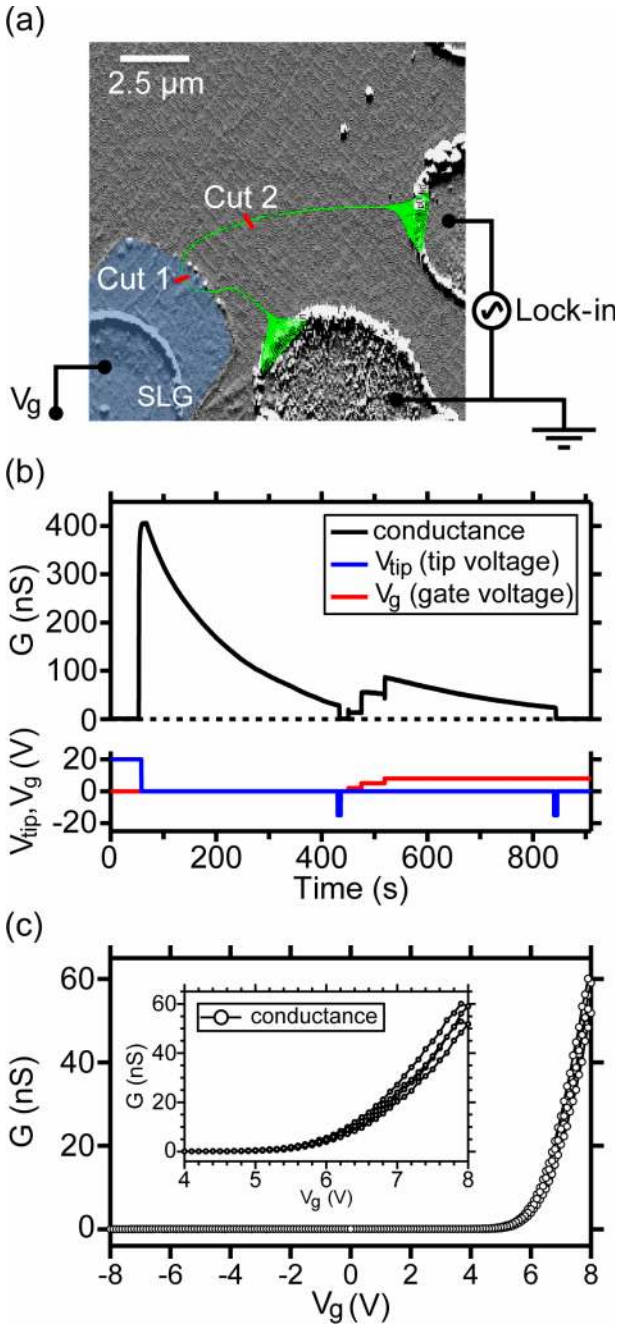

FIG. 4. C-AFM lithography on CVD-grown SLG/LAO/STO. (a) Schematic of lithography pattern overlaid on non-contact AFM image. A path connecting two electrodes crosses the SLG region. Two cuts, one on the graphene region and the other outside the graphene are executed after writing the nanowire. The SLG contacts a third Ti/Au electrode, which is used to bias the SLG. (b) Monitored conductance G, tip voltage V_{tip}, and gate voltage V_{g} versus time during the c-AFM lithography process. (c) Conductance G of the resultant GCO-FET action as a function of V_{g}.

conductance drops to zero as the tip crosses the written nanowire. Afterwards, tip voltage is kept at 0 (V_{tip} = 0 V), and increasingly, positive gate voltages are applied to the graphene (V_g = 2 V, 5 V, 8 V). The two-terminal conductance shows a discrete jump associated with the graphene voltage steps, demonstrating that the LAO/STO nanowire junction conductance can be modulated using the SLG top gate. At the end of the experiment, the nanowire circuit is cut ("cut 2," outside the graphene region), verifying that the conductance measured is taking place through the nanowire and not a

distinct parallel path. Fig. 4(c) shows the channel conductance of a similar nanowire device written over the same canvas only after cutting on the graphene region (similar to "cut 1"). The two-terminal conductance of the graphene/complex oxide field effect transistor (GCO-FET) channel as a function of graphene gate voltage shows a "turn-on" near V_g = 6 V (Figure 4(c) inset). The observation that the subsequent gate sweeps do not overlap reflects the time-dependent decay of the conductance of the LAO/STO nanowires.

In summary, it has been demonstrated that the metal-insulator transition of LAO/STO heterostructures can be controlled by c-AFM lithography in the presence of exfoliated or CVD-grown SLG. These hybrid materials are expected to produce a variety of novel phenomena owing to the rich behavior of each constituent system and the nanoscale control over the complex-oxide properties. Novel correlations, tunable THz plasmonic properties, and superconducting proximity effects are just a few of the possible new directions which are enabled by graphene/LAO/STO heterostructures.

This work is supported by ONR GCO N00014-13-1-0806 (C.B.E., P.K., and J.L.) and the National Science Foundation Nos. DMR-1234096 (C.B.E.) and DMR- 1104191 (J.L.).

[1] K. S. Novoselov, A. K. Geim, S. V. Morozov, D. Jiang, Y. Zhang, S. V. Dubonos, I. V. Grigorieva, and A. A. Firsov, Science **306**(5696), 666 (2004).
[2] Y. B. Zhang, Y. W. Tan, H. L. Stormer, and P. Kim, Nature **438**(7065), 201 (2005).
[3] K. S. Novoselov, Z. Jiang, Y. Zhang, S. V. Morozov, H. L. Stormer, U. Zeitler, J. C. Maan, G. S. Boebinger, P. Kim, and A. K. Geim, Science **315**(5817), 1379 (2007).
[4] A. K. Geim and K. S. Novoselov, Nat. Mater. **6**(3), 183 (2007).
[5] A. H. C. Neto, F. Guinea, N. M. R. Peres, K. S. Novoselov, and A. K. Geim, Rev. Mod. Phys. **81**(1), 109 (2009).
[6] J. Mannhart and D. G. Schlom, Science **327**(5973), 1607 (2010).
[7] A. Ohtomo and H. Y. Hwang, Nature **427**(6973), 423 (2004).
[8] S. Thiel, G. Hammerl, A. Schmehl, C. W. Schneider, and J. Mannhart, Science **313**(5795), 1942 (2006).
[9] N. Reyren, S. Thiel, A. D. Caviglia, L. F. Kourkoutis, G. Hammerl, C. Richter, C. W. Schneider, T. Kopp, A. S. Ruetschi, D. Jaccard, M. Gabay, D. A. Muller, J. M. Triscone, and J. Mannhart, Science **317**(5842), 1196 (2007).
[10] A. D. Caviglia, S. Gariglio, N. Reyren, D. Jaccard, T. Schneider, M. Gabay, S. Thiel, G. Hammerl, J. Mannhart, and J. M. Triscone, Nature **456**(7222), 624 (2008).
[11] A. Brinkman, M. Huijben, M. Van Zalk, J. Huijben, U. Zeitler, J. C. Maan, W. G. Van der Wiel, G. Rijnders, D. H. A. Blank, and H. Hilgenkamp, Nat. Mater. **6**(7), 493 (2007).
[12] L. Li, C. Richter, J. Mannhart, and R. C. Ashoori, Nat. Phys. **7**(10), 762 (2011).
[13] D. A. Dikin, M. Mehta, C. W. Bark, C. M. Folkman, C. B. Eom, and V. Chandrasekhar, Phys. Rev. Lett. **107**(5), 056802 (2011).
[14] J. A. Bert, B. Kalisky, C. Bell, M. Kim, Y. Hikita, H. Y. Hwang, and K. A. Moler, Nat. Phys. **7**(10), 767 (2011).
[15] F. Bi, M. Huang, S. Ryu, H. Lee, C. W. Bark, C. B. Eom, P. Irvin, and J. Levy, Nat. Commun. **5**, 5019 (2014).
[16] M. B. Shalom, M. Sachs, D. Rakhmilevitch, A. Palevski, and Y. Dagan, Phys. Rev. Lett. **104**(12), 126802 (2010).
[17] A. D. Caviglia, M. Gabay, S. Gariglio, N. Reyren, C. Cancellieri, and J. M. Triscone, Phys. Rev. Lett. **104**(12), 126803 (2010).
[18] Y. W. Xie, Y. Hikita, C. Bell, and H. Y. Hwang, Nat. Commun. **2**, 494 (2011).
[19] R. Arras, V. G. Ruiz, W. E. Pickett, and R. Pentcheva, Phys. Rev. B **85**(12), 125404 (2012).
[20] N. Y. Chan, M. Zhao, N. Wang, K. Au, J. Wang, L. W. H. Chan, and J. Y. Dai, ACS Nano **7**(10), 8673 (2013).
[21] V. T. Tra, J. W. Chen, P. C. Huang, B. C. Huang, Y. Cao, C. H. Yeh, H. J. Liu, E. A. Eliseev, A. N. Morozovska, J. Y. Lin, Y. C. Chen, M. W. Chu, P. W. Chiu, Y. P. Chiu, L. Q. Chen, C. L. Wu, and Y. H. Chu, Adv. Mater. **25**(24), 3357 (2013).
[22] M. Huijben, G. Koster, M. K. Kruize, S. Wenderich, J. Verbeeck, S. Bals, E. Slooten, B. Shi, H. J. A. Molegraaf, J. E. Kleibeuker, S. van Aert, J. B. Goedkoop, A. Brinkman, D. H. A. Blank, M. S. Golden, G. van Tendeloo, H. Hilgenkamp, and G. Rijnders, Adv. Funct. Mater. **23**(42), 5240 (2013).
[23] C. Cen, S. Thiel, G. Hammerl, C. W. Schneider, K. E. Andersen, C. S. Hellberg, J. Mannhart, and J. Levy, Nat. Mater. **7**(4), 298 (2008).
[24] C. Cen, S. Thiel, J. Mannhart, and J. Levy, Science **323**(5917), 1026 (2009).
[25] A. Levy, F. Bi, M. Huang, S. Lu, M. Tomczyk, G. Cheng, P. Irvin, and J. Levy, J. Visualized Exp. **2014**(89), 51886 (2014).
[26] P. Irvin, M. Huang, F. J. Wong, T. D. Sanders, Y. Suzuki, and J. Levy, Appl. Phys. Lett. **102**(10), 103113 (2013).
[27] P. Irvin, Y. J. Ma, D. F. Bogorin, C. Cen, C. W. Bark, C. M. Folkman, C. B. Eom, and J. Levy, Nat. Photonics **4**(12), 849 (2010).
[28] Y. Ma, M. Huang, S. Ryu, C. W. Bark, C. B. Eom, P. Irvin, and J. Levy, Nano Lett. **13**(6), 2884 (2013).
[29] D. F. Bogorin, C. W. Bark, H. W. Jang, C. Cen, C. B. Eom, and J. Levy, Appl. Phys. Lett. **97**(1), 013102 (2010).
[30] G. L. Cheng, P. F. Siles, F. Bi, C. Cen, D. F. Bogorin, C. W. Bark, C. M. Folkman, J. W. Park, C. B. Eom, G. Medeiros-Ribeiro, and J. Levy, Nat. Nanotechnol. **6**(6), 343 (2011).
[31] X. Hong, K. Zou, A. M. DaSilva, C. H. Ahn, and J. Zhu, Solid State Commun. **152**(15), 1365 (2012).
[32] Y. Zheng, G. X. Ni, S. Bae, C. X. Cong, O. Kahya, C. T. Toh, H. R. Kim, D. Im, T. Yu, J. H. Ahn, B. H. Hong, and B. Ozyilmaz, Europhys. Lett. **93**(1), 17002 (2011).
[33] D. F. Jin, A. Kumar, K. H. Fung, J. Xu, and N. X. Fang, Appl. Phys. Lett. **102**(20), 201118 (2013).

[34] W. F. Andress, H. Yoon, K. Y. M. Yeung, L. Qin, K. West, L. Pfeiffer, and D. Ham, Nano Lett. **12**(5), 2272 (2012).
[35] C. W. Bark, D. A. Felker, Y. Wang, Y. Zhang, H. W. Jang, C. M. Folkman, J. W. Park, S. H. Baek, H. Zhou, D. D. Fong, X. Q. Pan, E. Y. Tsymbal, M. S. Rzchowski, and C. B. Eom, Proc. Natl. Acad. Sci. U.S.A. **108**(12), 4720 (2011).
[36] M. Huang, F. Bi, C. W. Bark, S. Ryu, K. H. Cho, C. B. Eom, and J. Levy, Appl. Phys. Lett. **104**(16), 161606 (2014).
[37] A. Gupta, G. Chen, P. Joshi, S. Tadigadapa, and P. C. Eklund, Nano Lett. **6**(12), 2667 (2006).
[38] M. Huang, F. Bi, S. Ryu, C. B. Eom, P. Irvin, and J. Levy, APL Mater. **1**(5), 052110 (2013).
[39] R. F. Schaufel and M. J. Weber, J. Chem. Phys. **46**(7), 2859 (1967).
[40] X. Li, W. Cai, J. An, S. Kim, J. Nah, D. Yang, R. Piner, A. Velamakanni, I. Jung, E. Tutuc, S. K. Banerjee, L. Colombo, and R. S. Ruoff, Science **324**(5932), 1312 (2009).
[41] J. F. Hsu, S. Dhingra, G. Jnawali, M. Huang, F. Bi, L. Chen, P. Irvin, C. B. Eom, J. Levy, and B. D'Urso, "Patterning, Transferring and Suspension of Single-layer Graphene by Deep-ultraviolet Lithography with a Single Thin Layer of Poly(methyl methacrylate)" (unpublished).